ABSTRACT

Title of Thesis: VIRAL INVESTIGATION OF REGULATORY HUMAN ASTROCYTES TO UNDERSTAND THE GLYMPHATIC SYSTEM

Paul Butz, Lucas Cheng, Riddhi Gopal, Anna Lin, Folarin Onifade, Robin Sultan

Directed By: Dr. Yanjin Zhang, D.V.M., MSc, Ph.D.
Associate Professor, Department of Veterinary Medicine
University of Maryland, College Park

Alzheimer's disease (AD), and other neurodegenerative diseases, results from an extracellular accumulation of beta-amyloid plaques, which are composed of misfolded peptide oligomers of beta-amyloid. The accumulation is thought to be due to the failure of the glymphatic system, a waste clearance system in brain, which uses aquaporin-4 (AQP4) protein water channels. This protein exists as heterotetramers of M1 and M23 isoforms from splice variants of AQP4. Previous studies suggested that Herpes Simplex Virus-1 (HSV-1) infection of the central nervous system (CNS) may be correlated to AD development. However, the effect of HSV-1 on the glymphatic system has not been definitively established. The objective of this study was to investigate HSV-1 infection on AQP4 expression in human brain-derived glial cells. Our preliminary results suggest that HSV-1 infection of the cells leads to lower protein levels of M23 isoform. These results suggest that HSV-1 infection may potentially interfere with the function of the glymphatic system through the reduction of the AQP4 protein.

VIRAL INVESTIGATION OF REGULATORY HUMAN ASTROCYTES TO UNDERSTAND THE GLYMPHATIC SYSTEM

By

Team VIRUS

Paul Butz
Lucas Cheng
Riddhi Gopal
Anna Lin
Folarin Onifade
Robin Sultan

Thesis submitted in partial fulfillment of the requirements of the Gemstone Program
University of Maryland, College Park
2018

Advisory Committee:
Dr. George A. Belov
Dr. Jeffrey DeStefano
Dr. Kara Duffy
Dr. Sabrina Kramer
Dr. Joshua D. Levin

Acknowledgements

We thank the Gemstone Honors Program for this incredible opportunity where we were able to grow as teammates and as individuals. We also thank our mentor, Dr. Yanjin Zhang, for his dedication and invaluable guidance that allowed us to overcome many challenges in research. For our progress in the lab, we also thank Liping Yang and other graduate students in the Department of Veterinary Medicine, who taught us research techniques. We express our thanks to Kelsey Corlett-Rivera, our team's librarian, for her commitment in providing thorough feedback throughout the past four years. We thank Dr. Prasanth Desai at Johns Hopkins University for his gift of the HSV-1 virus and Dr. Eugene Major from NIH for the gift of the SVG cell line. We thank our LaunchUMD fund donors: David and Julia Butz, Eileen Dugan, Mary Dugan, Deborah Eason, Rohit Gopal, and The Sultan Family.

Table of Contents

Table of Abbreviations

AD	Alzheimer's disease
Aβ	β-amyloid peptides
APP	β-amyloid precursor proteins
AQP	Aquaporin
AQP4	Aquaporin 4
CNS	Central Nervous System
CPE	Cytopathic Effect
CSF	Cerebrospinal fluid
DAPI	4',6-diamidino-2-phenylindole
FBS	Fetal bovine serum
HPI	Hours post-infection
HRP	Horseradish peroxidase
HSV-1	Herpes Simplex Virus Type 1
HSV-2	Herpes Simplex Virus Type 2
HSV1-tk	Herpes Simplex Virus Type 1 thymidine kinase
IFA	Immunofluorescence assay
ISF	Interstitial fluid
M1	M1 isoform tetramer
M23	M23 isoform tetramer
MEM	Minimum Essential Medium
MOI	Multiplicity of infection
OAP	Orthogonal arrays of particles
PBS	Phosphate buffered saline
PCR	Polymerase chain reaction
PSV	Pseudorabies virus
qPCR	Real-time PCR
RT	Reverse transcription
TLR2	Toll-like receptor 2
TLR9	Toll-like receptor 9
TNF	Tumor necrosis factor
TPM	Two-photon microscopy
WB	Western blotting

Chapter 1: Introduction

Alzheimer's disease (AD), a neurodegenerative disease, is characterized by low, irreversible deterioration of memory and cognitive function (Johanson et. al, 2008). While the cause of Alzheimer's disease is currently unknown, scientists have identified numerous physiological changes that occur during AD. The most notable of these physiological changes is the decreased clearance and degradation of the β-amyloid peptides whose buildup could result in an increased risk of developing plaques associated with neurodegenerative diseases (Strittmatter et. al, 1993). These β-amyloid peptide chains of 40-42 amino acids arise from the cleavage of β-amyloid precursor proteins (APP), which are transmembrane proteins expressed at high levels in the brain. APP can be metabolized by the action of secretases (α and γ) (Ehehalt et. al, 2003). When APP is metabolized by the intramembranous γ-secretase complex, it results in the production of β-amyloid peptides, which are typically deposited into the extracellular space or degraded in lysosomes (Ehehalt et. al, 2003). When the β-amyloids become internalized in a clathrin-coated endosomal compartment, they are folded into a β-pleated shape and form long aggregates called plaques (Ehehalt et. al, 2003). The plaques are deposited into the extracellular space following vesicle recycling (Ehehalt et. al, 2003). A study indicates that misfolded β-amyloid plaques can bind strongly to neurons and disrupt synapse connections that are important for neurotransmission and memory (Kim et al., 2013). Because of the deleterious health implications from the accumulation of β-amyloid plaques, it is important to understand the glymphatic system, which facilitates the removal of β-amyloid peptides to prevent the development of these plaques.

In healthy brains, the glymphatic system utilizes astrocytes in the central nervous system (CNS) to flush interstitial fluid[1] (ISF) through perivascular space, thus eliminating natural waste and byproducts generated from normal CNS functions (Thrane et al., 2014). The end feet of the astrocytes contain the water channel protein aquaporin-4 (AQP4), which is responsible for facilitating bulk flow of ISF to clear the β-amyloid from the cerebrospinal fluid (CSF) (Thrane et al., 2014). AQP4 is highly expressed in the brain and its main function is to remove β-amyloid peptides. Results from AQP4-knockout mice[2] experiments show that the deletion of AQP4 in the brain displays statistically significant reductions in clearance of β-amyloid peptides from the ISF (Iliff et al., 2012). Impaired function or decreased levels of AQP4 in the glymphatic system could lead to reduced clearance of β-amyloid peptides and therefore potentially contribute to the development of neurodegenerative diseases such as AD.

A functional decrease of the glymphatic system can also be caused by an alteration in the AQP4 localization. Researchers have studied the perivascular localization of AQP4 within postmortem frontal cortices and found that in individuals displaying signs of AD, the AQP4 localization was shifted from uniformly distributed throughout the cortical layers to varying amounts dependent on cortical layer depth (Zeppenfeld et al., 2017). This change in AQP4 localization to deeper cortical layers is also correlated with increased β-amyloid plaque within the postmortem brains of the AD

[1] ISF is a water based solvent in the body that bathes tissues and transports metabolic waste, nutrients, signaling molecules, and immune response molecules. It is found in between cells in what is known as tissue space (Wiig & Swartz, 2012).

[2] In AQP4-knockout mice, the AQP4 gene in the mouse DNA is disrupted by genetic engineering to eliminate the expression of AQP4 protein, which allows researchers to examine the function of AQP4 and the effects of its deletion (Iliff et al., 2012).

patients, which suggests the changes in AQP4 localization may be a contributing factor for the presence of β-amyloid plaques in the aged brain (Zeppenfeld et al., 2017).

AQP4 disruption affects the glymphatic system by decreasing its waste clearance function. However, the impact from viral infections of neuroglial cells on AQP4 or the glymphatic system is not well understood. The neuronal infection by Herpes Simplex Virus Type 1 (HSV-1) is suspected to be a risk factor for AD (Itzhaki et al., 1997; Itzhaki, 2014). HSV-1, a neurotropic double-stranded DNA virus, is widespread in human populations. This virus primarily infects humans through the oral mucosa, undergoing lytic replication (Lewandowski, Zimmerman, Denk, Porter, & Prince, 2002). In chronic infections, the newly produced HSV-1 particles can then enter sensory neurons, as well as microglia and astrocytes, and establish latency, with no visible symptoms or viral replication (Li et. al., 2011; Marques et al., 2006). Certain conditions, such as a weakened immune system from aging, stress, or immunosuppression, can result in reactivation of HSV-1 virus. One proposed mechanism is that HSV-1-induced inflammatory response might lead to disruption of the AQP4 in astrocytes.

The objective of our research was to study the effect of HSV-1 infection on AQP4 expression. In this study, we infected human brain-derived astrocytes with HSV-1 and our results suggest that HSV-1 infection might induce reduction of AQP4 protein level. We hypothesize that this downregulation is a result of decreasing AQP4 gene expression or increasing AQP4 protein degradation. There is no conclusive data about the relationship between HSV-1 infection and AQP4 RNA level. Further research is needed to examine the HSV-1 effect on AQP4 expression. Examining the effects of HSV-1 infection on AQP4 will provide insights on the potential effect of HSV-1 infection on the

glymphatic system, because an alteration in AQP4 could impact the removal of β-amyloid peptides and contribute to the development of AD.

Chapter 2: Literature Review

2.1 The Glymphatic System

2.1.1 Overview of the System

Like the complex network of the lymphatic system which removes metabolic waste products from the body, the recently discovered glymphatic system removes waste from the intercellular space within the brain. The glymphatic system uses perivascular channels, formed by astroglial cells around blood vessels, to cause bulk flow of CSF, which contains proteins and metabolites, out of the brain, as illustrated in Figure 1 (Johanson et al., 2008). The glial cells, specifically astrocytes, use projections known as end feet to form a network around the exterior of arteries and veins inside the brain – composing the blood brain barrier (Iliff et al., 2012). The end feet of the AQP4 help facilitate the bulk flow of CSF as it flows throughout the brain. The CSF is pumped through the brain along the channels surrounding arteries, where it is then collected and drained from the brain (Iliff et al., 2012). Astrocytes, a specific type of glial cells, play a crucial role in forming the structure of the glymphatic system. Astrocytic processes encompass 97% of all the vasculature in the CNS and form small channels that allow CSF to flow into the brain and around the blood vessels (Verkhratsky, Nedergaard, & Hertz, 2015). An improperly functioning glymphatic system could lead to negative outcomes including neurodegenerative diseases such as AD, Parkinson's, and Huntington's (Johanson et al., 2008).

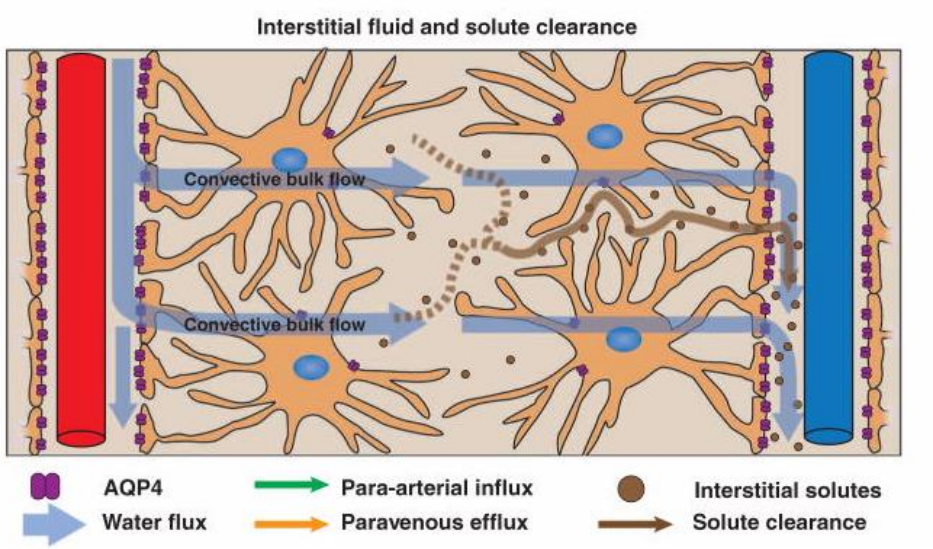

Figure 1. Diagram of the glymphatic system in the brain (Iliff et al., 2012).

When researchers studied the glymphatic system through two-photon microscopy (TPM) to locate fluorescent tracers in the brains of live mice, they found that hyperphosphorylated proteins, τ- and β-amyloid peptides, produced neurotoxic conditions that lead to AD (Nedergaard, 2013). These peptides are cleared by the flow of CSF and ISF through the glymphatic system. The aquaporin control the flow of the fluids which will determine the amount peptides removed. The peptides accumulate in the brain naturally, but the buildup of the peptides is what can lead to neurodegenerative diseases as they block synapse connections and interfere with memory (Palop & Mucke, 2010). The CSF and ISF flush the brain to rid it of these peptides. However, the glymphatic system of mice with AQP4 mislocated to astrocytic cell bodies does not clear as much soluble protein as mice with normal AQP4 water channels (Nedergaard, 2013). As a result, the β-amyloid-induced synaptic depression contributes to synaptic N-methyl-D-

aspartate (NMDA) receptor desensitization.[3] Any damage to this receptor can lead to weakened neurons and loss of normal memory function, which are physiological symptoms of AD and other neurodegenerative diseases (Palop & Mucke, 2010).

2.1.2 Aquaporin-4

Aquaporin (AQP) is a type of transmembrane protein that forms water channels for cells throughout the human body (Verkman, Phuan, Asavapanumas, & Tradtrantip, 2013). Many aquaporins have been found in glial cells such as AQP1, AQP3, AQP4, AQP5, AQP8, and AQP9 (Jung et al., 1994). AQP4 is found in the eyes, ears, skeletal muscle, kidney collecting muscle, and the membranes of the end feet of astrocytes in the CNS (Neely, 2001). The main function of AQP4 in the brain is to maintain water balance, neuroexcitation, and glial cell migration (Crane, Tajima, & Verkman, 2010).

Aquaporins that are comprised of six transmembrane alpha-helices form tetramers in pores allowing for water or other small molecules to pass through (Verkman, Phuan, Asavapanumas, & Tradtrantip, 2013). As water channel membrane proteins, aquaporins ensure water homeostasis, serve as transporters for osmosis, and in some cases, transport small polar solutes such as glycerol. AQP4 in astrocytic cell membrane is comprised of the same structure as other aquaporins. This protein plays a key role in the glymphatic system and the flow of CSF throughout the brain to remove β-amyloid peptides. Due to the important role of AQP4 in the glymphatic system, we were interested in the effect of HSV-1 infection on AQP4.

[3] NMDA is a glutamate receptor which facilitates calcium influx under depolarized conditions in the postsynaptic membrane. This channel is critical for the development of the CNS, neuroplasticity and memory processes (Blanke & VanDongen, 2009).

2.1.3 M1 and M23 Isoform Tetramers

AQP4 is composed of two isoforms, M1 and M23[4]. Of the two types, M1 is the full-length isoform of the protein that initiates translation at Met-1, while M23 is the shorter isoform starting at Met-23, due to alternative splicing (Jin et al., 2011; Tajima, Crane, & Verkman, 2010). The AQP4 assembles into an orthogonal array of particles (OAP), which are critical in the function of AQP4 as the size of the structural aggregates determines the rate of water movement (Silberstein et al., 2004). The size of this formation is determined by the ratio of M23:M1 tetramers. A greater ratio of M23:M1 tetramers produce larger OAPs (Crane, Tajima, & Verkman, 2010). A lower ratio of M23:M1 produces a smaller OAP as illustrated in Figure 2 (Jin et al., 2011). Ratios with more M23 isoforms create OAPs of greater than 100 particles while ratios with fewer M23 isoforms form small arrays of fewer than 12 particles (Crane, Tajima, & Verkman, 2010).

The OAP assembly size determines diffusion (Tajima, Crane, & Verkman, 2010). Previous studies have shown that changing the M23:M1 ratio has an effect on the OAP size and thus AQP4 function, as depicted in Figure 2 (B) (Jin, Rossi, & Verkman, 2011). Increasing the ratio greatly increases OAP size, while varying the ratio allowed for marked heterogeneity in OAP size (Jin, Rossi, & Verkman, 2011). Our research focused on the M23 isoform instead of the M1 isoform, because M23 amount determines the assembly size of OAPs (Tajima, Crane, & Verkman, 2010).

[4] New names are proposed for the M1 isoform as AQP4a and M23 tetramer as AQP4c. However, to establish consistency in the following discussion, the conventional terminology of M1 and M23 was maintained in this thesis (Potokar, Jorgačevski, & Zorec, 2016).

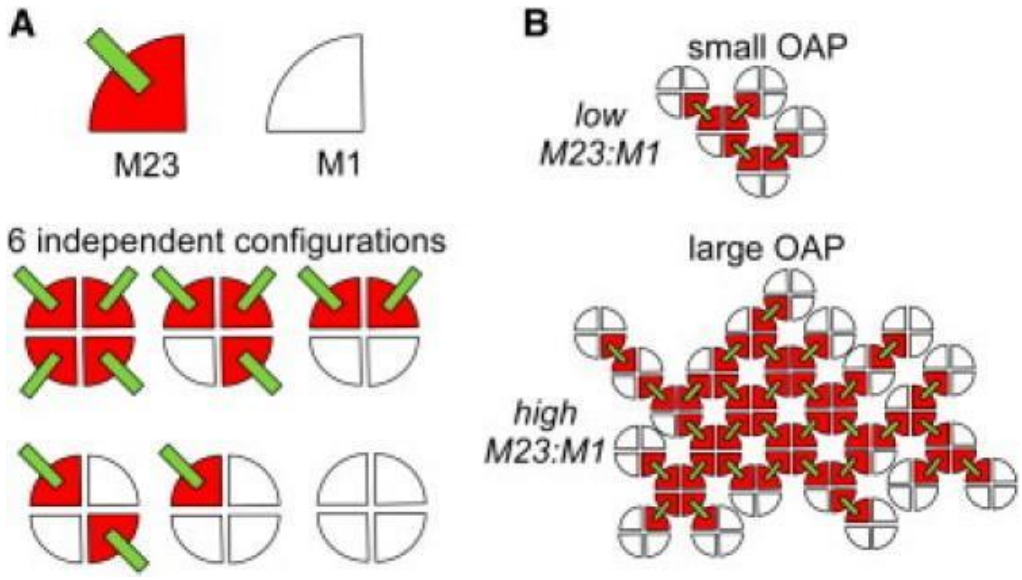

Figure 2. OAP assembly from AQP4 heterotetramers M1 and M23 isoforms. (a) Shows potential sites of the M23-M23 interactions as well as the possible AQP4 M1/M23 heterotetramers. (b) Changing the M23:M1 ratio affects the size of OAPs (Jin, Rossi, & Verkman, 2011).

2.2 Herpes Simplex Virus 1

2.2.1 Classification

There are three subfamilies in the family of *Herpesviridae*: *Alphaherpesvirinae*, *Betaherpesvirinae*, and *Gammaherpesvirinae* (Whitley, 1996). HSV-1 belongs to the *Alphaherpesvirinae* subfamily. Additional viruses in the *Alphaherpesvirinae* subfamily include varicella zoster virus (VZV), Herpes Simplex Virus 2 (HSV-2), and Pseudorabies Virus (PSV) (McGeoch & Cook, 1994). HSV-1 belongs to the genus *Simplexvirus.* The members of genus *Simplexvirus* have specific characteristics such as a short replicative cycle, a broad host range and latent infection in neurons (Whitley, 1996; International Committee on Taxonomy of Viruses, 9th Report, 2011). HSV-1 is a virus that only infects humans (McGeoch & Cook, 1994).

2.2.2 HSV-1 Structure

HSV-1 is an enveloped virus containing double stranded DNA (Grünewald et al., 2003). The overall structure of HSV-1 virions consists of three main components: the nucleocapsid, the tegument, and the lipid envelope, as depicted in Figure 3 (Grünewald et al., 2003).

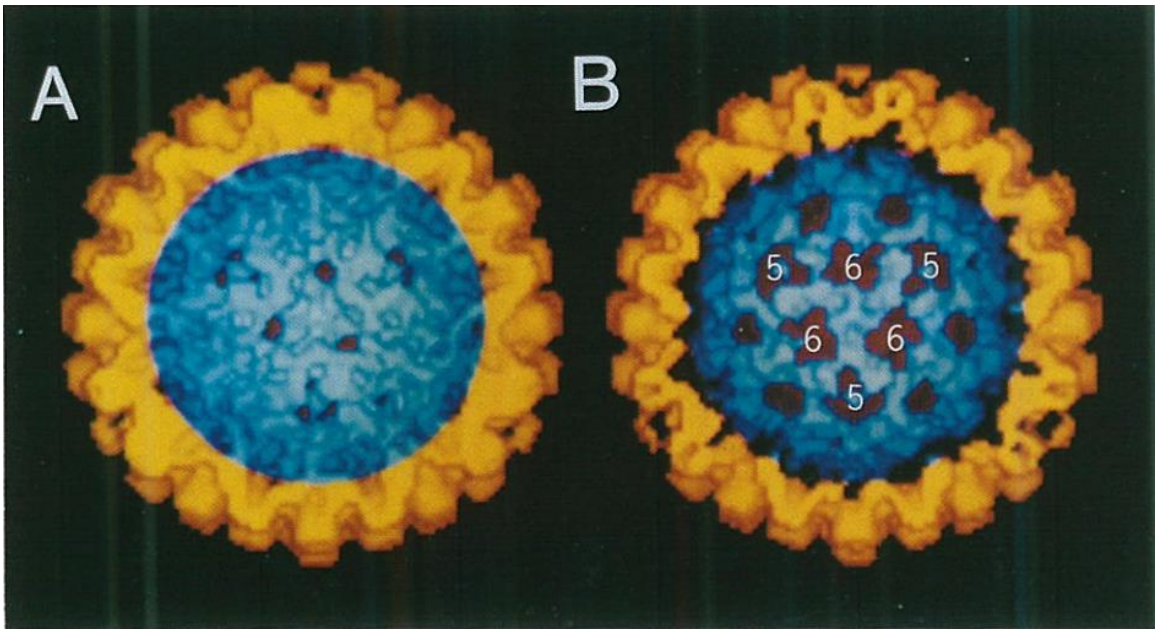

Figure 3. Surface representation for a three-fold view of HSV-1. (a) Shows the outer layer of the virus as well as the core. (b) The virus has both a 5- and 6-fold axis representing the density distribution (Schrag, Prasad, Rixon, & Chiu, 1989).

The HSV-1 nucleocapsid contains the genome of the virus and is icosahedral in structure. The virion is surrounded by the viral envelope that consists of a lipid bilayer and eleven documented glycoproteins that function in HSV-1 binding and interacting with host cells (Kelly, Fraefel, Cunningham, & Diefenbach, 2009). In between the viral envelope and the nucleocapsid is the tegument, which aids processes involved in viral replication (Kelly, Fraefel, Cunningham, & Diefenbach, 2009).

2.2.3 HSV-1 Replication

HSV-1 is transmitted orally between humans. The virus first infects the oral mucosa, a protective lining found in the mouth surrounding the oral cavity and the esophagus (Vorvick, 2014; Squier & Kremer, 2001).

To initiate infection, HSV-1 glycoproteins on the viral envelope bind to the host cell surface receptors (Turner, Bruun, Minson, & Browne, 1998). The viral envelope then fuses with the host cell membrane and allows the nucleocapsid to enter the cytoplasm with the help of multiple proteins from the tegument region. The nucleocapsid moves to the perinuclear area and releases the viral genome into the nucleus. HSV-1 replication occurs in a specific order in gene expression: immediate-early genes, early genes, and late genes (Whitley, 1996). The immediate-early genes encode regulatory proteins. The early genes encode enzymes for replicating viral DNA. The late genes encode structural proteins for virion packaging and assembly (Whitley, 1996). Virions are then released from the cell through exocytosis. This is the lytic cycle of HSV-1 and the process is shown in Figure 4, which depicts the HSV-1 life cycle in three stages.

After infecting the oral mucosa, HSV-1 can enter sensory nerve endings and infect the sensory neurons, where it enters latent infection with no visible symptoms or viral replication (Knipe et al., 2007). However, HSV-1 can be reactivated and cause the characteristic recurrent cold sores (Vorvick, 2014).

Studies have indicated that HSV-1 can hijack exosomal pathways to ensure its survival and persistence (Gallo, et al., 2017). The virus could use the extracellular vesicles as mediators for intercellular communication and microenvironment

modifications. Hence, HSV-1 causes a persistent[5] infection that remains in the host for life.

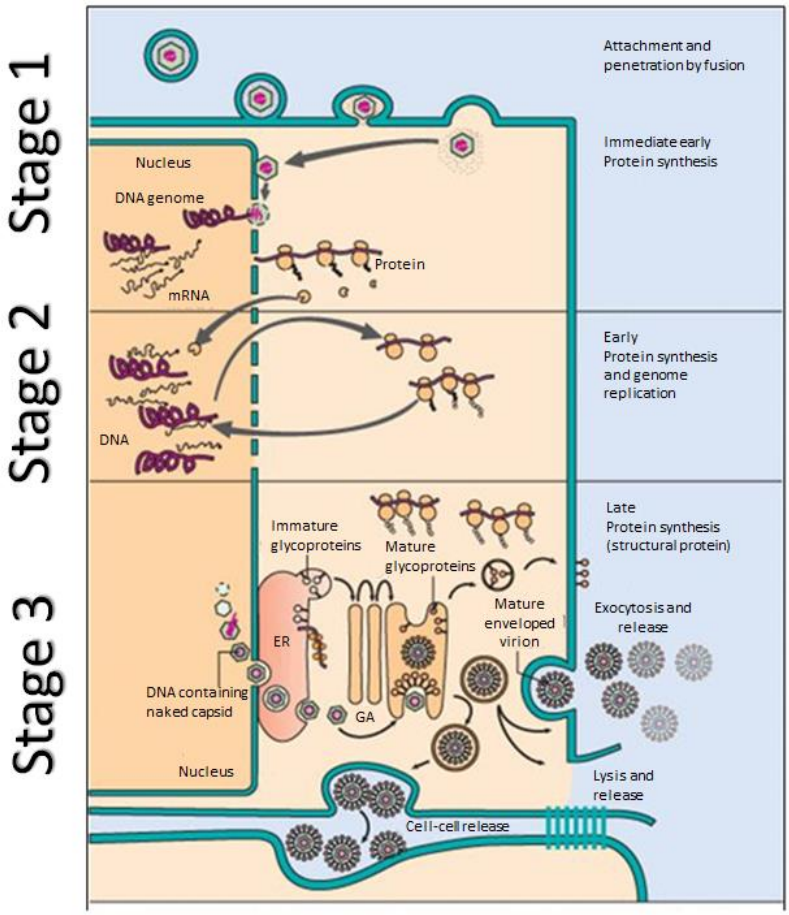

Figure 4. Illustration of the HSV-1 life cycle in three stages. The cycle begins with the attachment and entry of the virus, and ends with the exocytosis of newly replicated viruses (Murray, Rosenthal, & Pfaller, 2005).

2.2.4 Epidemiology

In the U.S., an estimated 51% of the population over the age of 12 tested positive for HSV-1 and approximately 90% of adults have been exposed to the virus, most of whom are infected by age 20 (Xu et al., 2002; Vorvick, 2014). Approximately 16% of

[5] Persistent viral infections occur when certain viruses enter a host and are never fully removed from the host body. Persistent viruses can exist in the host body as a latent, chronic, or slow infection (Boldogh, Albrecht, & Porter, 1996).

the population tested positive for both HSV-1 and HSV-2 (Xu et al., 2002). Among the people who tested positive for HSV-2, 76% were also tested positive for HSV-1 (Xu et al., 2002).

HSV-1 infection is incurable because if a person is infected, he or she will carry the virus for life, though some may not experience any symptoms (WHO, 2017). HSV-1 infection can lead to either mild or acute symptoms, which are well recognized as blisters or rashes around the mouth (Vorvick, 2014).

HSV-1 is spread through both direct contact from an infected person's saliva from activities such as kissing, and indirect contact from sharing items that come in contact with the infected saliva (CDC, 2014). HSV-1 is transmitted from neuronal axons to epidermal cells, where they then spread into the mucosal membranes for transmission to a new host (Mikloska & Cunningham, 2001). Another mode of transmission could be by indirect or direct contact with open herpes sore (Vorvick, 2014).

2.2.5 Pathogenesis

When HSV-1 enters the neuron, the viral replication can enter a latent phase where the virus remains present but is inactive. When microglial cells[6] detect the presence of HSV-1 through the pattern recognition receptors TLR2 or TLR9, these cells release small signaling proteins called cytokines, such as interferons and tumor necrosis factors (TNF). They trigger a response to control HSV-1 replication and inhibit the reactivation of HSV-1 (Sørensen et al., 2008).

[6] Microglial cells are located in the central nervous system (CNS) that comprise around 20% of all glial cells, with microglia maintaining brain homeostasis and acting as an immune defense for the brain (Kreutzberg, 1995).

At a later time, spontaneously or based on certain factors[7], the virus can exit the latency phase, reactivate, and attack the host body again. Though a healthy immune system may be able to inhibit HSV-1 and keep the virus in its latency phase, when the system is compromised and HSV-1 is allowed to reactivate, the virus can enter the CNS in some rare cases and cause Herpesviral encephalitis[8] (Conrady, Drevets, & Carr, 2009). Of these cases, there is a reported 70% mortality rate in untreated patients and 30% mortality rate in treated patients (Yao et al., 2014). Thus, while the symptoms of HSV-1 may seem harmless, they can result in major health implications. HSV-1 is not just limited to neurons; these viruses also infect other cell types including astrocytes (Li et al., 2011).

It is theorized that infected glial cells allow for HSV-1 to efficiently replicate and spread over the CNS. Astrocytes, in particular, are highly susceptible to HSV-1 infections (Li et. al., 2011; Marques et al., 2006). In a mouse model, it is reported that during the acute phase of HSV-1 encephalitis, there is a 35% downregulation in AQP4 mRNA level at 7 days post infection, and 2.9-fold upregulation at 6 month post infection (Torres et al., 2007).

Previous studies suggest that chronic HSV-1 infection may be a risk factor for the development of neurodegenerative diseases later in life, though there is no significant experimental evidence of HSV-1's role as a pathogenic co-factor in AD (Beffert, Bertrand, Champagne, Gauthier, & Poirier, 1998). HSV-1 is normally latent in aged

[7] Factors include fear, emotional stress, exposure to ultraviolet light, immunosuppression, chemotherapy, and many other factors (Scott, Coulter, Biagioni, O'Neill, & Lamey, 1997).

[8] Herpesviral encephalitis is a viral infection of the CNS that results in encephalitis, which is an inflammation of the brain that has severe consequences on the infected patients such as seizures, headaches, change in behavior, and even brain damage and death (National Institute of Neurological Disorders and Stroke [NINDS], 2015).

brains but can potentially be reactivated during stress and immunosuppression, causing damage in the brain (Itzhaki et al., 1997; Wozniak et al., 2005). Reactivated HSV-1 can cause direct and inflammatory damage, probably due to the accumulation of β-amyloid (Aβ) and of AD-like tau (P-tau) (Itzhaki et al., 1997; Wozniak et al., 2005). Additionally, HSV-1 DNA has been found to be localized in amyloid plaques in AD (Wozniak et al., 2009). There are other harmful effects of infection including HSV-1 interaction with APP, resulting in HSV-1 and APP being transported together in the cell (Cheng et al., 2011). Furthermore, reactivation of the virus in brains could occur because of the response of toll-like receptors (TLRs) in HSV-1 infected astrocytes (Martin et al., 2014). This HSV-1 reactivation is correlated with neuroinflammation and neurodegenerative markers (phospho-tau and TauC3) (Martin et al., 2014). Despite the studies that implicate HSV-1 infection in neurodegeneration to the subsequent development of AD, a definitive link between HSV-1 infection and AD is not established. It is therefore necessary to investigate the impact of HSV-1 infection on astrocytes of the glymphatic system, which is implicated in the onset of neurodegenerative diseases.

Chapter 3: Methodology

The major objective of this study was to assess the impact of HSV-1 infection on the function and the production level of AQP4 with specific interest in the M23 isoform. This study was not meant to research the enzymatic processes of the glymphatic system. The effect of HSV-1 on AQP4 was studied to contribute to a broader understanding of the glymphatic system. The relationship between HSV-1 infection and AQP4 downregulation was tested through the assessment of AQP4 protein levels in infected

cells by Western blot (WB) analysis, visualization of AQP4 localization using immunofluorescence assay (IFA), and the quantification of AQP4 RNA level through reverse transcription and real time polymerase chain reaction (RT-qPCR).

3.1 Cell Culture, HSV-1 Infection, Virus Titration

The human fetal glial cell line, SVG, was a gift from Dr. Eugene Major of NIH (Major & Yacante, 1989). SVG cells were used, rather than neuroglial cells from aged brains as the former may have fewer possible confounding variables that are often found in the latter. The cell confluency remains high, between 80-90%, before infection. This cell line was maintained with Minimum Essential Medium (MEM) supplemented with 10% fetal bovine serum (FBS). The cells were incubated at 37ºC with 5% CO_2. The cells in a T-25 flask were designated for maintenance and growth whereas cells in a 10 cm diameter Petri dish were designated for storage in liquid nitrogen.

When passaging, the cells were washed three times with 1000 mL of phosphate buffered saline (PBS) to remove dead cells and FBS, then detached from the culture flask with 500 mL of trypsin. The cells were then incubated for two minutes to allow time for the trypsin enzyme to detach the cells from the culture flask. A portion of the detached cells were then plated into wells of culture plates and incubated for next-day infection, if the cells reached 90% confluency. In order to infect the SVG cells, the HSV-1-GFP virus stock was diluted to reach the desired multiplicity of infection (MOI) (Lin, Yang, & Zhang, 2018; Ma, Yang, & Zhang, 2018). HSV-1-GFP virus was a gift from Dr. Prashant Desai of Johns Hopkins University (Desai and Person, 1998). The MOI levels varied in the experiments; however, we commonly used the MOIs of 0.1, 0.5, 1.0, and 5.0 in this study. Infected cells were harvested at varying time-points as stated in results or

figure legends. Longer incubation time was needed to assess protein level change of AQP4 with WB. Therefore, infected cells for WB were harvested between 9 hours post infection (hpi) and 48 hpi in this study.

3.2 Quantification of AQP4 RNA Expression

At the specified hpi, the cells were harvested using TRIzol Reagent (Thermo Fisher Scientific). Total RNA was isolated from the cell lysate according to the manufacturer's instructions and established methodologies (Lin, Yang, & Zhang, 2018; Ma, Yang, & Zhang, 2018). Once isolated, the RNA was used in reverse transcription (RT) with a combination of oligo(dT) primers and random hexamers to synthesize cDNA and ensure all targets of interest were equally represented in the subsequent analysis. The cDNA was subjected to a real-time PCR (qPCR) analysis as previously described (Yang et al., 2016). The primers in qPCR are ICP0-F1 (5'-CATGCACCGCTTCTGCATCC-3') and ICP0-R1 (5'-CGTCACGCCCACTATCAGGT-3') for the detection of HSV-1; RR-AQP4-F1 (5'- TCACCATGGTTCATGGAAAT-3') and RR-AQP4-R1 (5'-CAGTCCGTTTGGAATCACAG-3') were used for the detection of AQP4. Transcripts of hRPL32, a housekeeping gene, were also detected for control as described (Yang et al., 2016). HSV-1 ICP0 plasmid (a gift from Dr. Qiyi Tang at Howard University) was used in the qPCR to obtain an HSV-1 standard curve to assess absolute ICP0 RNA copies. As there should not be an HSV-1 related decrease in the transcript level of hRPL-32, AQP4 RNA level was assessed and shown as relative level after normalization with hRPL-32.

3.3 Western Blotting

Total proteins in cell lysate samples were separated by SDS-PAGE and analyzed by Western blotting to identify AQP4, as described previously (Yang et al., 2016). The Western blotting was done in three steps: first, separating the proteins by size; second, transferring the protein from the gel to a nitrocellulose membrane; and third, detecting the target protein using a corresponding primary antibody followed by a secondary antibody conjugated with horseradish peroxidase (HRP) (Yang et al., 2016). The primary antibodies used in this study were against AQP4 (B-5) (Santa Cruz Biotechnology, Inc., Dallas, TX) and beta-tubulin (Sigma). Mouse anti-HSV-1 gD monoclonal antibody (DL6) conjugated with HRP (Santa Cruz) was used for the detection of HSV-1 gD in a 1:1000 dilution. The chemiluminescence substrate was used to reveal the presence of HRP-conjugated antibody on the membrane. The chemiluminescence signal acquisition and densitometry analysis were conducted using the Quantity One program (v4.6) and a Chemi-Doc XRS imaging system (Bio-Rad Laboratories, Hercules, CA). The WB analysis provided us with relative protein levels in comparison to controls, though not an absolute measurement of the amount of target protein present in each sample (Yang et al., 2016).

3.4 Immunofluorescence Assay (IFA)

IFA was conducted as previously described (Lin, Yang, & Zhang, 2018; Ma, Yang, & Zhang, 2018). SVG cells were grown on cover glass slips in a 12-well culture plate. The cells were fixed with 1% paraformaldehyde for 15 minutes at room temperature. The AQP4 antibody was diluted at 1:50 ratio and applied onto the cover

glass, followed by incubation at 37ºC for 30 minutes. Diluted goat anti-mouse IgG-fluorescein isothiocyanate (FITC) conjugate (Sigma, St. Louis, MO) was then added to the cover glass followed by incubation at 37ºC for 30 minutes. The 4',6-diamidino-2-phenylindole (DAPI) was used to stain the DNA in the nucleus of the cells. The cover glass was mounted onto slides using SlowFade Gold antifade reagent (Thermo Fisher) and observed under fluorescence microscopy. The ZEISS Axiovert200M inverted fluorescence microscope and Axio Vision program were then used to image, process, and analyze the IFA slides.

IFA was used to assess AQP4 expression and its location in the presence and absence of HSV-1 infection. This technique was applied to ensure that the changes in AQP4 expression or location were indeed due to HSV-1 infection.

Chapter 4: Results

4.1 Optimization of HSV-1 Inoculation Amount and Infection Time

Prior to analyzing the effects of HSV-1 infection on AQP4, the optimal infection time and MOI of HSV-1-GFP were determined by the observation of green fluorescence from HSV-1-GFP and cytopathic effect (CPE). The time point/MOI combinations with high virus infection rate and low CPE were selected for additional experiments. The titer of the HSV-1-GFP stock was determined by limiting dilution and titration in Vero cells for TCID50 (Yang et al., 2016). SVG cells were initially infected with HSV-1-GFP at the MOI of 1.0 and 5.0. The cells were imaged under fluorescence microscopy at 24 and 48 hpi. Compared to the mock-infected cells, the HSV-1-GFP infected cells displayed lower cell density as shown in the phase contrast image (Figures 5a & 5c). At 24 hpi,

cells inoculated with an MOI of 5.0 displayed a higher number of positive fluorescence cells than those with an MOI of 1.0 (Figure 5a). At 48 hpi, the difference in positive fluorescence between different MOI levels is less noticeable. However, higher cell death is observed in the 48 hpi sample infected with 5.0 MOI rather than 1.0 MOI. Compared to cells harvested at 24 hpi (Figure 5a), the 48 hpi cells (Figure 5c) had a higher rate of fluorescence-positive cells in both 1.0 MOI and 5.0 MOI-wells. Based on the CPE at 24 and 48 hpi (Figures 5a and 5c), 1.0 MOI inoculum was commonly used for SVG cell infection in our experiments. In addition, infected cells at 48 hpi (Figure 5c) demonstrated a reduction in cell morphology quality and density. Both infected wells displayed increased number of dead cells than that of their 24 hpi counterpart. Therefore, cells were harvested before 48 hpi in the following tests.

SVG cells were infected at an MOI of 0.1, 0.5, and 1.0 to further optimize the inoculum using WB analysis. The cells were harvested at 24 and 48 hpi and mock-infected cells were included for comparison. WB results showed an increase in HSV-1-GFP gD level with an increase in MOI, while the tubulin protein level remained unchanged (Figure 5b). The same trend was observed for 48 hpi samples, except the protein level for 1.0 MOI appears equivalent to 0.5 MOI (Figure 5d). Additionally, HSV-1 GFP gD level is higher at 48 hpi than 24 hpi as shown in Figure 5.

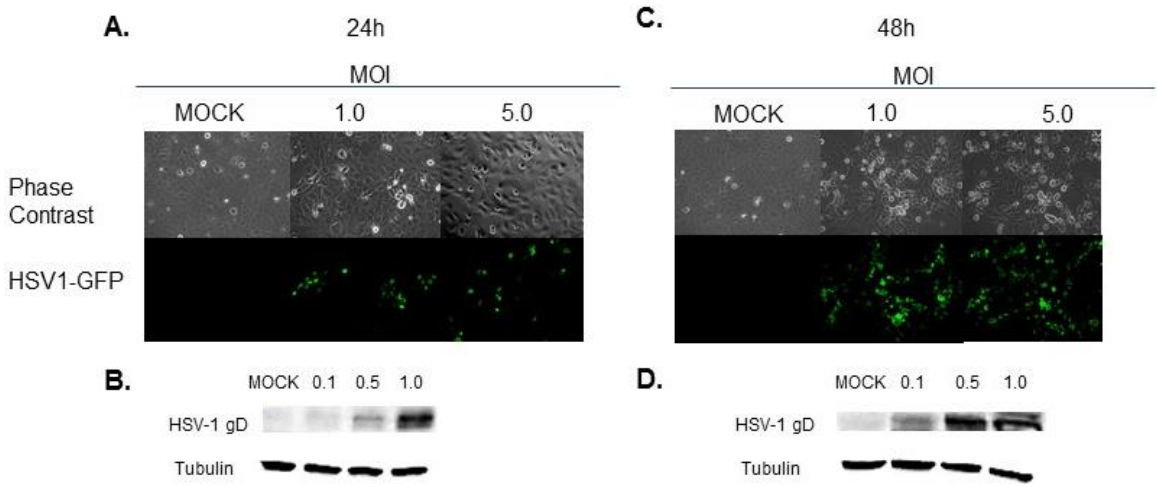

Figure 5. HSV-1-GFP infection rate increases with time and MOI. (a) Fluorescence microscopy at 24 hpi displays the presence of HSV-1-GFP infection shown in green fluorescence at 200x magnification. (b) Increase in HSV-1 gD level along with incremental MOI-detected by Western blot analysis of 24 hpi samples at 200x magnification. (c) Fluorescence and phase contrast microscopy at 48 hpi indicate higher rate HSV-1-GFP infection, lower cell confluency, and more dead SVG cells than at 24 hpi. Increased number of dead cells present in infected wells at 48 hpi while few dead cells observed in mock-infected wells. (d) Western Blot analysis demonstrates increase in HSV-1-GFP gD protein level along with MOI at 48 hours.

4.2 HSV-1 Induces Reduction of AQP4 Protein

To analyze the effect of HSV-1 on AQP4 protein level, we infected SVG cells with HSV-1-GFP at the MOIs of 1.0, 5.0, and 10. Figures 6a and 6b display our preliminary results that suggest AQP4 protein level decreased along with MOI increase and extended infection time. In Figure 6a, AQP4 appears to be present as two bands, corresponding to 30/32 kDa. The top band is assumed to be the M1 isoform (32 kDa) and the bottom band is the M23 isoform (30 kDa) (Rossi et al., 2009). Compared with mock-infected cells, the M1 isoform band in the infected cells showed minimal change, while the M23 isoform band decreased. This decrease in protein level is more apparent between mock-infected and 1.0 MOI infected cells. M23 band strength appears roughly similar across the infection levels. Yet, the tubulin level unexpectedly reduced in the cells with 5.0 and 10 MOI.

In Figure 6b, the temporal kinetics of AQP4 in HSV-infected cells were examined. Compared to the mock-infected cells, HSV-infected cells appeared to have lower AQP4 levels at 24, 36, and 48 hpi. In cells infected with the MOI of 5.0, AQP4 level was lower than the cells with an MOI of 1.0. The mock-infected cells had no observable change in AQP4 between 24 hpi and 48 hpi. Tubulin band strength is roughly constant at each time point and MOI, however, a slight decrease is observed at 5.0 MOI in the 24 hpi sample. This dip in band intensity can be attributed to a loading error when conducting the experiment. Further study is needed to confirm the AQP4 protein level change in HSV-infected cells.

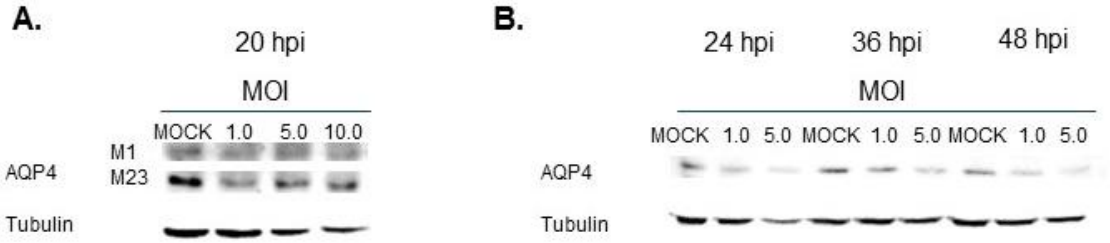

Figure 6. AQP4 protein levels decrease relative to tubulin, a housekeeping protein, in infected SVG samples. (a) Western blot analysis shows that AQP4 decreases in HSV-infected cells. (b) Western blot analysis examines AQP4 protein level in infected SVG samples from 24 to 48 hpi.

4.3 AQP4 RNA Level in HSV-infected Cells is Inconclusive

We attempted to determine the AQP4 transcript level in HSV-infected cells. The SVG cells were infected with different MOI and harvested at different hpi. Infected cells designated for RT-qPCR tests were harvested at shorter time points between 2 and 9 hpi. The time points were shortened to check the early levels of AQP4 after infection.

Results from multiple experiments were not consistent due to various reasons, including technical errors in RNA isolation, RT, and qPCR that are described in further detail in the discussion. The high discrepancies in qPCR results made the experiment

inconclusive and further work is needed to elucidate the effects of HSV-1-GFP infection on AQP4 transcript level.

4.4 Probable Altered Pattern of AQP4 in HSV-infected Cells

Immunofluorescence assay was used to determine whether AQP4 localization experienced a shift in HSV-infected cells in comparison to mock-infected cells. The IFA images suggest that in mock-infected cells, AQP4 seemed to be evenly distributed throughout the cells (Figures 7a and 7b). In HSV-infected cells, the AQP4 seemed to have a different distribution pattern from the mock-infected cells (Figure 7). As a wide-field fluorescence microscope was used to observe the IFA slide and take photos, the exact distribution pattern was difficult to conclude. Repeated tests and confocal microscopy are needed to further examine the AQP4 subcellular location. In addition, the images were adjusted separately to show the subcellular location pattern shift, which did not reflect the relative protein levels as indicated by the WB.

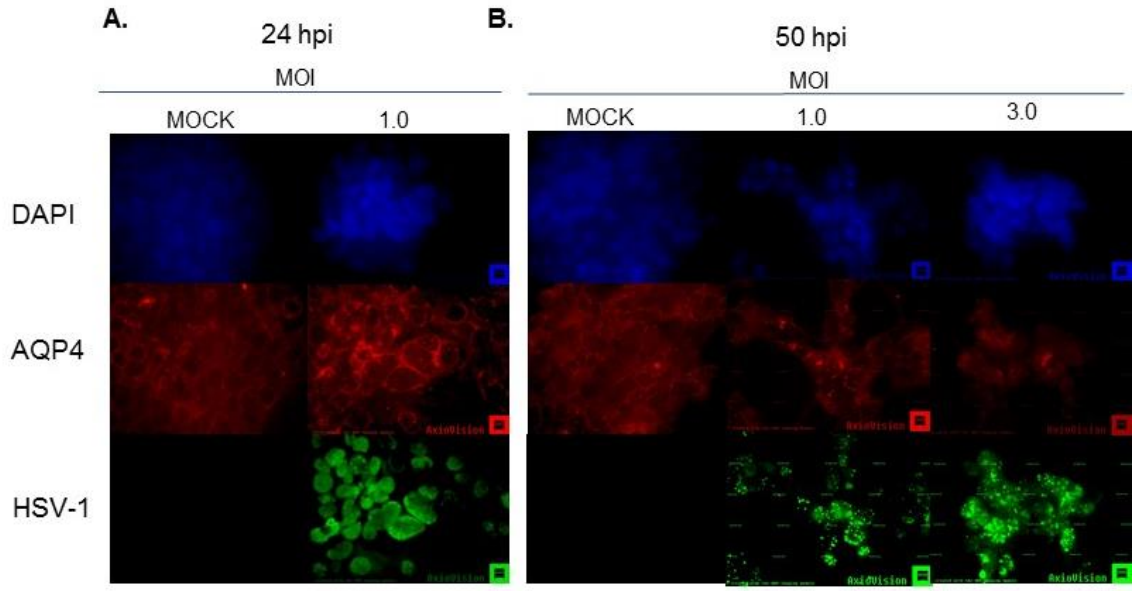

Figure 7. Immunofluorescence assay displays the location of AQP4 in HSV-infected SVG cells. (a) IFA images of 24 hpi sample. DAPI (blue) AQP4 (red), and HSV-1-GFP (green) are shown. (b) Location of AQP4 protein at 48 hpi for Mock, 1.0 MOI and 3.0 MOI.

Chapter 5: Discussion

A functioning glymphatic system is crucial for the removal of β-amyloid peptides and waste from the brain. AQP4 is involved in ISF and CSF exchanges in the glymphatic system in the brain. In this study, we have obtained preliminary data that suggests HSV-1 induces AQP4 downregulation. Optimization of HSV-1 virus inoculum and infection time indicates that SVG cells inoculated at an MOI of 0.1 and 1.0 and harvested between 24 and 48 hpi were best for the study as shown in Figure 5.

The preliminary results of this study indicate HSV-1 infection of SVG cells might lead to downregulation of AQP4. Figure 6b showed that AQP4 was reduced in HSV-infected cells, whereas tubulin protein had minimum change. This suggests that downregulation of AQP4 by HSV-1 is not due to its universal downregulation of all cellular proteins. Whereas M1 isoform level stayed relatively consistent, the M23 isoform level decreased in the infected cells. Despite not seeing a dose-dependent

decrease in AQP4, Figure 6a indicates the M23 isoform experiences a decrease in the presence of infection. Because M23 isoform plays a major role in AQP4 tetramer formation, an alteration in the ratio between M23 and M1 following HSV-1 infection could impact the rate of waste removal in the glial cells. However, further studies must be conducted to confirm our observations in the virus-infected cells.

In a previous study of HSV-1 induced encephalitis in mice, there is a mild reduction of AQP4 RNA transcript in the acute phase of infection and an up-regulation in the long term (Torres et al., 2007). However, our data regarding AQP4 RNA level is inconclusive as we lack replicability in our results. Though multiple trials were conducted to assess the impact of HSV-1 infection on AQP4 transcripts, errors such as weak amplification curves indicating poor RNA quality and evidence of cross-contamination between samples rendered the results unreliable. Though inconclusive, our initial result suggests HSV-1 infection does not influence AQP4 transcript level. If this observation were confirmed, lower AQP4 protein levels in HSV-infected cells could be attributed to changes at the protein level rather than the RNA level.

Our IFA results suggest that the AQP4 pattern in HSV-infected cells was probably altered, which could potentially affect AQP4 function as well. Zeppenfeld et al. (2017) concluded that AQP4 localization shifts towards deep cortical layers in AD patients. It is possible that HSV-1 infection might induce AQP4 subcellular location change, however, further studies must be conducted to confirm the observation. Our use of widefield microscopy instead of confocal microscopy could account for the less clear IFA images.

Despite our effort and the volume of data we have gathered, the experiments must be repeated to confirm our observations. A majority of our results reflect qualitative data that could not be quantified or statistically analyzed. Quantification of protein bands in WB analysis through the QuantityOne program produced inconclusive results due to the weakness of the bands. Additionally, results obtained through RT-qPCR were omitted from this study due to lack of replicability and variation between samples due to human error (e.g. HSV-1 transcripts detected in mock samples). As a result, statistical analysis and error bars did not reflect accurate trends in data obtained.

Some other possible sources in error for our research include cell contamination and discrepancies in techniques between group members. In regards to cell contamination, the SVG cells experienced a recurring fungal infection due to unknown reasons. Proper personal protective equipment was required at all times and proper sterilization techniques were followed. However, based on the high rate of contamination, it became evident that the team's efforts to follow the aseptic techniques required in handling cells were not sufficient. To mediate this issue, in the late stage of the study, the team relied on a graduate student, Liping Yang to maintain SVG cells on our behalf. All of our procedures and data are stored in a shared Google Drive folder for any team member to reference to alleviate variation in technique. These were often cross-checked with our principal investigator and the graduate students in the lab to ensure accuracy.

Chapter 6: Conclusion

Our research investigated the impact of HSV-1 infection on AQP4, a protein critical to the proper functioning of the glymphatic system. Decreased clearance of β-amyloid peptides by a malfunctioning glymphatic system can lead to an increased risk of developing neurodegenerative diseases such as AD (Strittmatter et. al, 1993).

We studied the effects of HSV-1 infection on AQP4 by infecting cells at varying MOI. Western blotting and IFA were used to assess protein level, visualize protein localization, and confirm HSV-1 infection. Although our results are currently inconclusive, parts of our data offer clues as to how HSV-1 affects AQP4 protein. We have demonstrated, as seen in Figure 5, that AQP4 protein was reduced by HSV-1 infection. Based on the preliminary results, higher MOI and longer infection time could result in further reduction of AQP4. These results suggest that HSV-1 is potentially able to reduce AQP4 and consequently modulate the glymphatic system. If the AQP4 protein were significantly reduced, the bulk ISF and CSF flow would slow down and the rate of clearance would decrease considerably. This slower removal could lead to the harmful β-amyloid plaque build-up, which can in turn trigger neurodegenerative disease. Understanding how viral infection can alter the waste clearance pathway in the brain may facilitate the development of treatment strategies targeting these pathways.

Future research on HSV-1 effect on AQP4 is warranted as our observations need to be confirmed with repeated experiments. The effect of HSV-1 on AQP4 transcript needs to be studied to determine if AQP4 protein reduction is due to a transcript level change. If not, one of the experiments to test for the protein level degradation is to use proteasome inhibitor MG132 (Yang et al., 2016). This test would assess if the ubiquitin-

proteasome degradation pathway is used to degrade AQP4 in HSV-1 infected cells. If this follow-up test has positive results, it will indicate that AQP4 reduction is due to degradation by the ubiquitin-proteasome pathway. Upon identifying the molecular mechanisms *in vitro*, further research could include *in vivo* tests to assess the effects of HSV-1 infection on the glymphatic system and its function as a whole. An animal model would also provide a more realistic and therefore improve model in assessing the prevalence of HSV-1 infection in astrocytes and whether its effect on AQP4 would be severe. Future extensions from this project could have major impacts on understanding the molecular process by which the glymphatic system functions including how the AQP4 change by HSV-1 infection induces its malfunction and consequently the development of neurodegenerative diseases.

References

Alzheimer's Association. (2015). *2015 Alzheimer's Disease: Facts and figures*. Retrieved from http://www.alz.org/facts/downloads/facts_figures_2015.pdf

Arduino, P. G., & Porter, S. R. (2008). Herpes Simplex Virus Type 1 infection: overview on relevant clinico-pathological features. *Journal of Oral Pathology & Medicine*, *37*(2), 107–121. http://doi.org/10.1111/j.1600-0714.2007.00586.

Beffert, U., Bertrand, P., Champagne, D., Gauthier, S., & Poirier, J. (1998). HSV-1 in brain and risk of Alzheimer's disease. The Lancet, 351(9112), 1330–1331. https://doi.org/10.1016/S0140-6736(05)79057-7

Blanke, M. L., & VanDongen, A. M. J. (2009). Activation Mechanisms of the NMDA Receptor. In A. M. Van Dongen (Ed.), *Biology of the NMDA Receptor*. Boca Raton (FL): CRC Press/Taylor & Francis. Retrieved from http://www.ncbi.nlm.nih.gov/books/NBK5274/

Boldogh, I., Albrecht, T., & Porter, D. D. (1996). Persistent Viral Infections. In S. Baron (Ed.), *Medical Microbiology* (4th ed.). Galveston (TX): University of Texas Medical Branch at Galveston. Retrieved from http://www.ncbi.nlm.nih.gov/books/NBK8538/

Camassa, L. M. A., Lunde, L. K., Hoddevik, E. H., Stensland, M., Boldt, H. B., De Souza, G. A., … Amiry-Moghaddam, M. (2015). Mechanisms underlying AQP4 accumulation in astrocyte endfeet. *Glia*, *63*(11), 2073-2091. http://doi.org/10.1002/glia.22878

Cheng, S.-B., Ferland, P., Webster, P., and Bearer, E. L. (2011). Herpes simplex virus dances with amyloid precursor protein while exiting the cell. *PLoS One* 6:e17966. http://doi.org/10.1371/journal.pone.0017966

Conrady, C. D., Drevets, D. A., & Carr, D. J. J. (2010). Herpes simplex type I (HSV-1) infection of the nervous system: Is an immune response a good thing? *Journal of Neuroimmunology*, *220*(1–2), 1–9. http://doi.org/10.1016/j.jneuroim.2009.09.013

Crane, J. M., Tajima, M., & Verkman, A. S. (2010). Live-Cell imaging of Aquaporin-4 diffusion and interactions in orthogonal arrays of particles. *Neuroscience*, *168*(4), 892–902. https://doi.org/10.1016/j.neuroscience.2009.08.034

Desai, P., & Person, S. (1998). Incorporation of the green fluorescent protein into the herpes simplex virus type 1 capsid. *Journal of Virology*, *72*(9), 7563–8. Retrieved from https://www.ncbi.nlm.nih.gov/pubmed/9696854

Ehehalt, R., Keller, P., Haass, C., Thiele, C., & Simons, K. (2003). Amyloidogenic processing of the Alzheimer β-amyloid precursor protein depends on lipid rafts. The Journal of Cell Biology, 160(1), 113–123. https://doi.org/10.1083/jcb.200207113

Gallo, A., Vella, S., Miele, M., Timoneri, F., Di Bella, M., Bosi, S., … Conaldi, P. G. (2017). Global profiling of viral and cellular non-coding RNAs in Epstein-Barr virus-induced lymphoblastoid cell lines and released exosome cargos. Cancer Letters, 388, 334–343. https://doi.org/10.1016/j.canlet.2016.12.003

Genital Herpes - CDC Fact Sheet (Detailed). (2014). Center for Disease Control and Prevention. Retrieved from http://www.cdc.gov/std/herpes/stdfact-herpes-detailed.htm

Grünewald, K., Desai, P., Winkler, D. C., Heymann, J. B., Belnap, D. M., Baumeister, W., & Steven, A. C. (2003). Three-Dimensional Structure of Herpes Simplex Virus

from Cryo-Electron Tomography. *Science*, *302*(5649), 1396–1398. https://doi.org/10.1126/science.1090284

Iliff, J. J., Wang, M., Liao, Y., Plogg, B. A., Peng, W., Gundersen, G. A., … Nedergaard, M. (2012). A paravascular pathway facilitates CSF flow through the brain parenchyma and the clearance of interstitial solutes, including Amyloid β. *Science Translational Medicine*, *4*(147). https://doi.org/10.1126/scitranslmed.3003748

International Committee on Taxonomy of Viruses, 9th Report. (2011). Herpesviridae. Retrieved from https://talk.ictvonline.org/ictv-reports/ictv_9th_report/dsdna-viruses-2011/w/dsdna_viruses/91/herpesviridae

Itzhaki, R. F., Lin, W., Shang, D., Wilcock, G. K., Faragher, B., and Jamieson, G. A. (1997). Early reports herpes simplex virus type 1 in brain and risk of Alzheimer's disease. *Lancet.* 349, 241–244. http://doi.org/10.1016/S0140-6736(96)10149-5

Johanson CE, Duncan J, Klinge PM, et al. Multiplicity of cerebrospinal fluid functions: New challenges in health and disease. Cerebrospinal Fluid Res. 2008;5:10. doi: 10.1186/1743-8454-5-10.

Jin, B., Rossi, A., & Verkman, A. S. (2011). Model of Aquaporin-4 supramolecular assembly in orthogonal arrays based on heterotetrameric association of M1-M23 isoforms. *Biophysical Journal*, *100*(12), 2936–2945. https://doi.org/10.1016/j.bpj.2011.05.012

Jung, J. S., Bhat, R. V., Preston, G. M., Guggino, W. B., Baraban, J. M., & Agre, P. (1994). Molecular characterization of an aquaporin cDNA from brain: candidate osmoreceptor and regulator of water balance. *PNAS*, *91*(26), 13052–13056. https://doi.org/10.1073/pnas.91.26.13052

Kelly, B. J., Fraefel, C., Cunningham, A. L., & Diefenbach, R. J. (2009). Functional roles of the tegument proteins of herpes simplex virus type 1. *Virus Research*, *145*(2), 173–186. http://doi.org/10.1016/j.virusres.2009.07.007

Kim, T., Vidal, G., Djurisic, M., William, C., Birnbaum, M., Garcia, K., … Shatz, C. (2013). Human LilrB2 is a β-amyloid receptor and its murine homolog PirB regulates synaptic plasticity in an Alzheimer's model. *Science*, *341*(6152), 1399–1404. https://doi.org/10.1126/science.1242077.

Knipe, D. M., Howley, P. M., Griffen, D., Martin, M., Lamb, R., Roizman, B., & Straus, S. (2007). *Fields' Virology* (Vol. 1). Lippincott Williams & Wilkins.

Kreutzberg, G. W. (1995). Microglia, the first line of defence in brain pathologies. *Arzneimittel-Forschung*, *45*(3A), 357–360.

Lewandowski, G., Zimmerman, M. N., Denk, L. L., Porter, D. D., & Prince, G. A. (2002). Herpes simplex type 1 infects and establishes latency in the brain and trigeminal ganglia during primary infection of the lip in cotton rats and mice. *Archives of Virology*, *147*(1), 167–179.

Li, J., Hu, S., Zhou, L., Ye, L., Wang, X., Ho, J., & Ho, W. (2011). Interferon lambda inhibits herpes simplex virus type I infection of human astrocytes and neurons. *Glia*, *59*(1), 58–67. http://doi.org/10.1002/glia.21076

Lin, S., Yang, L., & Zhang, Y.-J. (2018). Hepatitis E Virus: Isolation, propagation, and quantification. *Current Protocols in Microbiology*, *48*(1), 15L.1.1-15L.1.15. https://doi.org/10.1002/cpmc.50

Ma, Z., Yang, L., & Zhang, Y.-J. (2018). Porcine reproductive and respiratory syndrome virus: Propagation and quantification. *Current Protocols in Microbiology*, *48*(1), 15M.1.1-15M.1.14. https://doi.org/10.1002/cpmc.51

Major, E. O., & Yacante, D. A. (1989). Human Fetal Astrocytes in Culture Support the Growth of the Neurotropic Human Polyomavirus, JCV. *Journal of Neuropathology & Experimental Neurology*, *48*(4), 425–436. https://doi.org/10.1097/00005072-198907000-00004

Martin, C., Aguila, B., Araya, P., Vio, K., Valdivia, S., Zambrano, A., et al. (2014). Inflammatory and neurodegeneration markers during asymptomatic HSV-1 reactivation. *J. Alzheimers Disease.* 39, 849–859. http://doi.org/10.3233/JAD-131706

Marques, C. P., Hu, S., Sheng, W., & Lokensgard, J. R. (2006). Microglial cells initiate vigorous yet non-protective immune responses during HSV-1 brain infection. *Virus Research*, *121*(1), 1–10.http://doi.org/10.1016/j.virusres.2006.03.009

McGeoch, Duncan J., & Cook, Simon. (1994). Molecular phylogeny of the Alphaherpesvirinae subfamily and a proposed evolutionary timescale. *Journal of Molecular Biology*, *238*(1), 9-22. https://doi.org/10.1006/jmbi.1994.1264

Mikloska, Z., & Cunningham, A. (2001). Alpha and gamma interferons inhibit herpes simplex virus type 1 infection and spread in epidermal cells after axonal transmission. *Journal of Virology*, *75*(23), 11821–26. https://doi.org/10.1128/JVI.75.23.11821-11826.2001

Murray, P., Rosenthal, K., & Pfaller, M. (2005). *Medical Microbiology - 5th Edition* (5th ed.). Retrieved from https://www.elsevier.com/books/medical-microbiology/murray/978-0-323-03303-9

Nedergaard, M. (2013). Garbage truck of the brain. *Science*, *340*(6140), 1529–1530. http://doi.org/10.1126/science.1240514

Neely JD, Christensen BM, Nielsen S, Agre P. Heterotetrameric composition of aquaporin- water channels. Biochemistry 1999;38:11156–63.

Neely JD, Amiry-Moghaddam M, Ottersen OP, Froehner SC, Agre P, Adams ME. Syntrophin-dependent expression and localization of Aquaporin-4 water channel protein. Proc. Natl. Acad. Sci. USA 2001;98:14108–13.

NINDS. (2017). Meningitis and encephalitis fact sheet. Retrieved from https://www.ninds.nih.gov/Disorders/Patient-Caregiver-Education/Fact-Sheets/Meningitis-and-Encephalitis-Fact-Sheet

Palop, J. J., & Mucke, L. (2010). Amyloid-β-induced neuronal dysfunction in Alzheimer's disease: from synapses toward neural networks. *Nature Neuroscience*, *13*(7), 812–818. http://doi.org/10.1038/nn.2583

Potokar, M., Jorgačevski, J., & Zorec, R. (2016). Astrocyte aquaporin dynamics in health and disease. *International Journal of Molecular Sciences*, *17*(7), 1121. https://doi.org/10.3390/ijms17071121

Rossi, A., Pisani, F., Nicchia, G. P., Svelto, M., & Frigeri, A. (2009). Evidence for a leaky scanning mechanism for the synthesis of the shorter M23 protein isoform of Aquaporin-4. *The Journal of Biological Chemistry*, *285*(7), 4562–4569. https://doi.org/10.1074/jbc.M109.069245

Schrag, J. D., Prasad, B. V. V., Rixon, F. J., & Chiu, W. (1989). Three-dimensional structure of the HSV1 nucleocapsid. *Cell*, *56*(4), 651–660. https://doi.org/10.1016/0092-8674(89)90587-4

Scott, D. A., Coulter, W. A., Biagioni, P. A., O'Neill, H., & Lamey, P.-J. (1997). Detection of herpes simplex virus type 1 shedding in the oral cavity by polymerase chain reaction and enzyme-linked immunosorbent assay at the prodromal stage of recrudescent herpes labialis. *Journal of Oral Pathology & Medicine*, *26*(7), 305–309. https://doi.org/10.1111/j.1600-0714.1997.tb00220.x

Silberstein, C., Bouley, R., Huang, Y., Fang, P., Pastor-Soler, N., Brown, D., & Van Hoek, A. (2004). Membrane organization and function of M1 and M23 isoforms of aquaporin-4 in epithelial cells. *American Journal of Physiology Renal Physiology*, *287*(3), F501–F511. https://doi.org/10.1152/ajprenal.00439.2003

Squier, C. A., & Kremer, M. J. (2001). Biology of oral mucosa and esophagus. *JNCI Monographs*, *2001*(29), 7–15.

Sørensen, L. N., Reinert, L. S., Malmgaard, L., Bartholdy, C., Thomsen, A. R., & Paludan, S. R. (2008). TLR2 and TLR9 synergistically control herpes simplex virus infection in the brain. *Journal of Immunology (Baltimore, Md.: 1950)*, *181*(12), 8604–8612.

Strittmatter, W. J., Saunders, A. M., Schmechel, D., Pericak-Vance, M., Enghild, J., Salvesen, G. S., & Roses, A. D. (1993). Apolipoprotein E: high-avidity binding to beta-amyloid and increased frequency of type 4 allele in late-onset familial Alzheimer disease. Proceedings of the National Academy of Sciences, 90(5), 1977–1981. https://doi.org/10.1073/pnas.90.5.1977

Tajima, M., Crane, J. M., & Verkman, A. S. (2010). Aquaporin-4 (AQP4) associations and array dynamics probed by photobleaching and single-molecule analysis of green fluorescent protein-AQP4 chimeras. *The Journal of Biological Chemistry*, *285*(11), 8163–8170. https://doi.org/10.1074/jbc.M109.093948

Thrane AS, Rangroo Thrane V, Nedergaard M. Drowning stars: reassessing the role of astrocytes in brain edema. Trends Neurosci. 2014;37:620–628. doi: 10.1016/j.tins.2014.08.010.

Torres, M., F. J., Völcker, D., Dörner, N., Lenhard, T., Nielsen, S., Haas, J., … Meyding-Lamadé, U. (2007). Aquaporin 4 regulation during acute and long-term experimental Herpes simplex virus encephalitis. *Journal of Neurovirology*, *13*(1), 38–46. http://doi.org/10.1080/13550280601145340

Turner, A., Bruun, B., Minson, T., & Browne, H. (1998). Glycoproteins gB, gD, and gHgL of Herpes Simplex Virus Type 1 Are Necessary and Sufficient To Mediate Membrane Fusion in a Cos Cell Transfection System. *Journal of Virology*, *72*(1), 873–875.

Verkhratsky, A., Nedergaard, M., & Hertz, L. (2014). Why are Astrocytes Important? *Neurochemical Research*, *40*(2), 389–401. http://doi.org/10.1007/s11064-014-1403-2

Verkman, A. S., Phuan, P., Asavapanumas, N. and Tradtrantip, L. (2013), AQP4 and AQP4-IgG in NMO. *Brain Pathology*, *23*, 684-695. doi:10.1111/bpa.12085

Vorvick, L. (2014). Herpes - oral: MedlinePlus Medical Encyclopedia. Retrieved April 20, 2018, from https://www.nlm.nih.gov/medlineplus/ency/article/000606.htm

Whitley, R. J. (1996). Herpesviruses. In S. Baron (Ed.), *Medical Microbiology* (4th ed.). Galveston (TX): University of Texas Medical Branch at Galveston. Retrieved from http://www.ncbi.nlm.nih.gov/books/NBK8157/

WHO. (2017). Herpes simplex virus. Retrieved from http://www.who.int/mediacentre/factsheets/fs400/en/#hsv1

Wiig, H., & Swartz, M. (2012). Interstitial fluid and lymph formation and transport: physiological regulation and roles in inflammation and cancer. *Physiological Reviews*, *92*(3), 1005–1060. https://doi.org/10.1152/physrev.00037.2011

Wozniak, M. A., Mee, A. P., and Itzhaki, R. F. (2009). Herpes simplex virus type 1 DNA is located within Alzheimer's disease amyloid plaques. *J. Pathol.* 217, 131–138. doi: 10.1002/path.2449

Wozniak, M. A., Shipley, S. J., Combrinck, M., Wilcock, G. K., and Itzhaki, R. F. (2005). Productive herpes simplex virus in brain of elderly normal subjects and Alzheimer's disease patients. *J. Med. Virol.* 75, 300–306. doi: 10.1002/jmv.20271

Xu, F., Schilinger, J. A., Sternberg, M. R., Johnson, R. E., Lee, F. K., Nahmias, A. J., & Markowitz, L. E. (2002). Seroprevalence and coinfection with Herpes Simplex Virus Type 1 and Type 2 in the United States, 1988–1994. *The Journal of Infectious Diseases*, *185*(8), 1019–1024. https://doi.org/10.1086/340041

Yang, L., Wang, R., Ma, Z., Xiao, Y., Nan, Y., Wang, Y., … Zhang, Y.-J. (2016). Porcine Reproductive and Respiratory Syndrome Virus Antagonizes JAK/STAT3 Signaling via Nsp5 by Inducing STAT3 Degradation. *Journal of Virology*, *91*(3), JVI.02087-16. https://doi.org/10.1128/JVI.02087-16

Yao, H. -W., Ling, P., Tung, Y. –Y., Hsu, S. -M., & Chen, S. -H. (2014). In Vivo Reactivation of Latent Herpes Simplex Virus 1 in Mice Can Occur in the Brain before Occurring in the Trigeminal Ganglion. *Journal of Virology*, *88*(19), 11264–11270. http://doi.org/10.1128/JVI.01616-14

Zeppenfeld, D., Simon, M., Haswell, J., D'Abreo, D., Murchison, C., Quinn, J., … Iliff, J. (2017). Association of perivascular localization of Aquaporin-4 with cognition and Alzheimer Disease in aging brains. *JAMA Neurology*, *74*(1), 91–9. https://doi.org/10.1001/jamaneurol.2016.4370